DARK MATTER

ASTR 333/433

TODAY

BARS & SPIRAL STRUCTURE
THIN & THICK DISKS
GALAXY MERGERS

Homework 1
Due Thursday

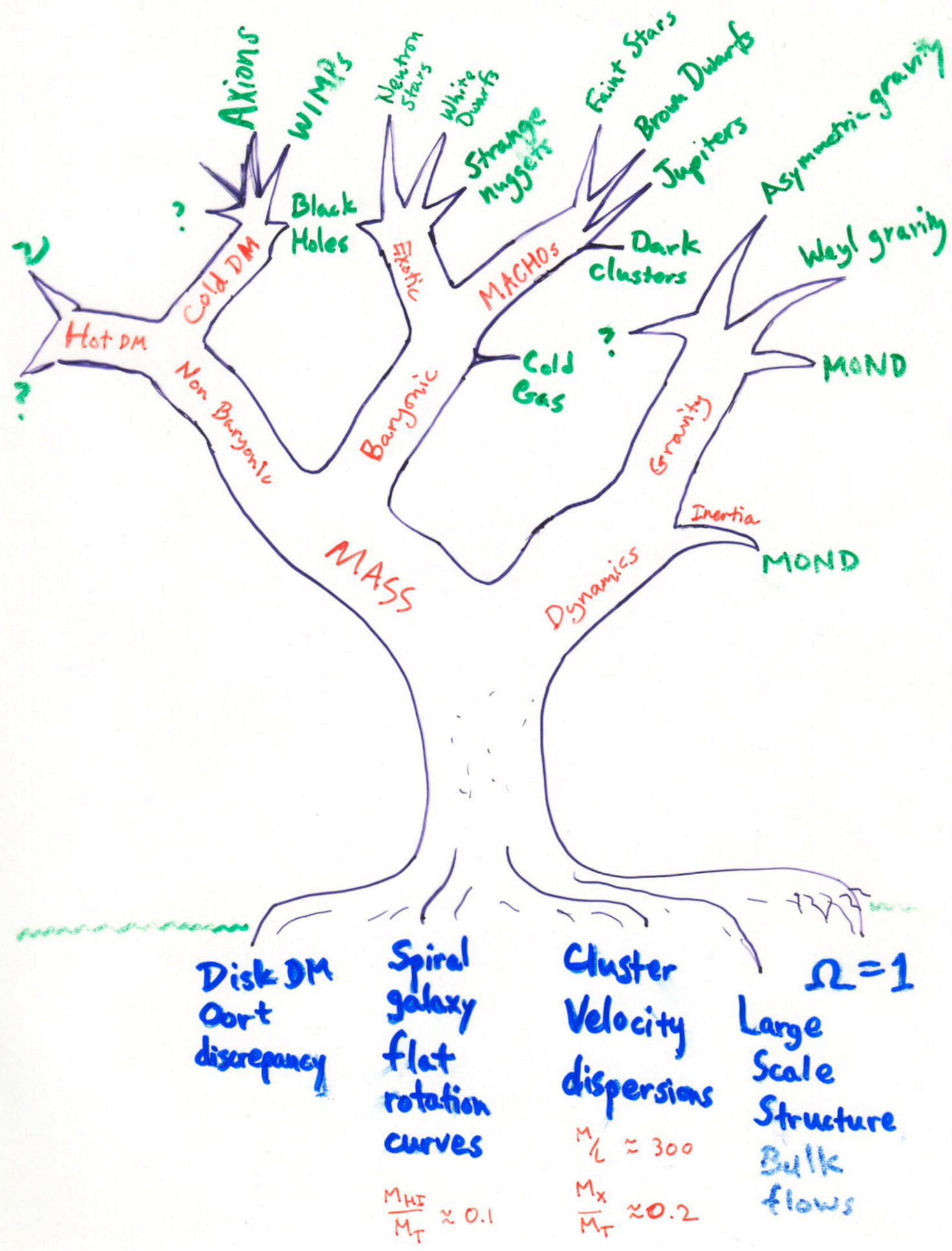

Bars

- Non-axis-symmetric potential
  - provides perturbing torque to orbits
- Transfer angular momentum
  - stars get outward kick
  - gas sinks toward center
- Interact with dark matter halo
  - live halos may encourage bar growth, but
  - dynamical friction slows bars

gas is compressed & shocks along leading edge of bar

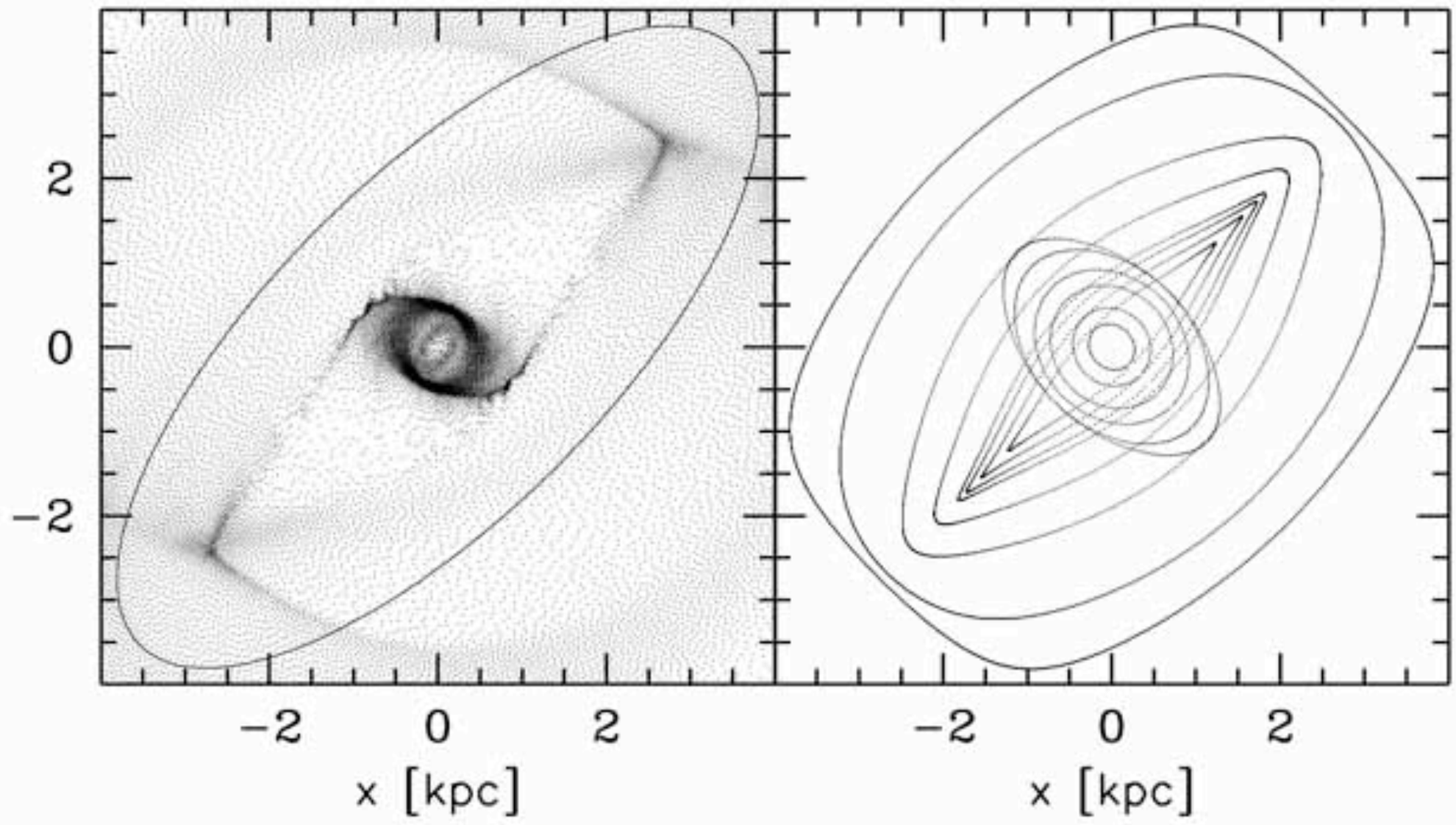

Fig 5.33 'Galaxies in the Universe' Sparke/Gallagher CUP 2007

Closed orbits in the frame of a bar rotating with pattern speed Ω_B

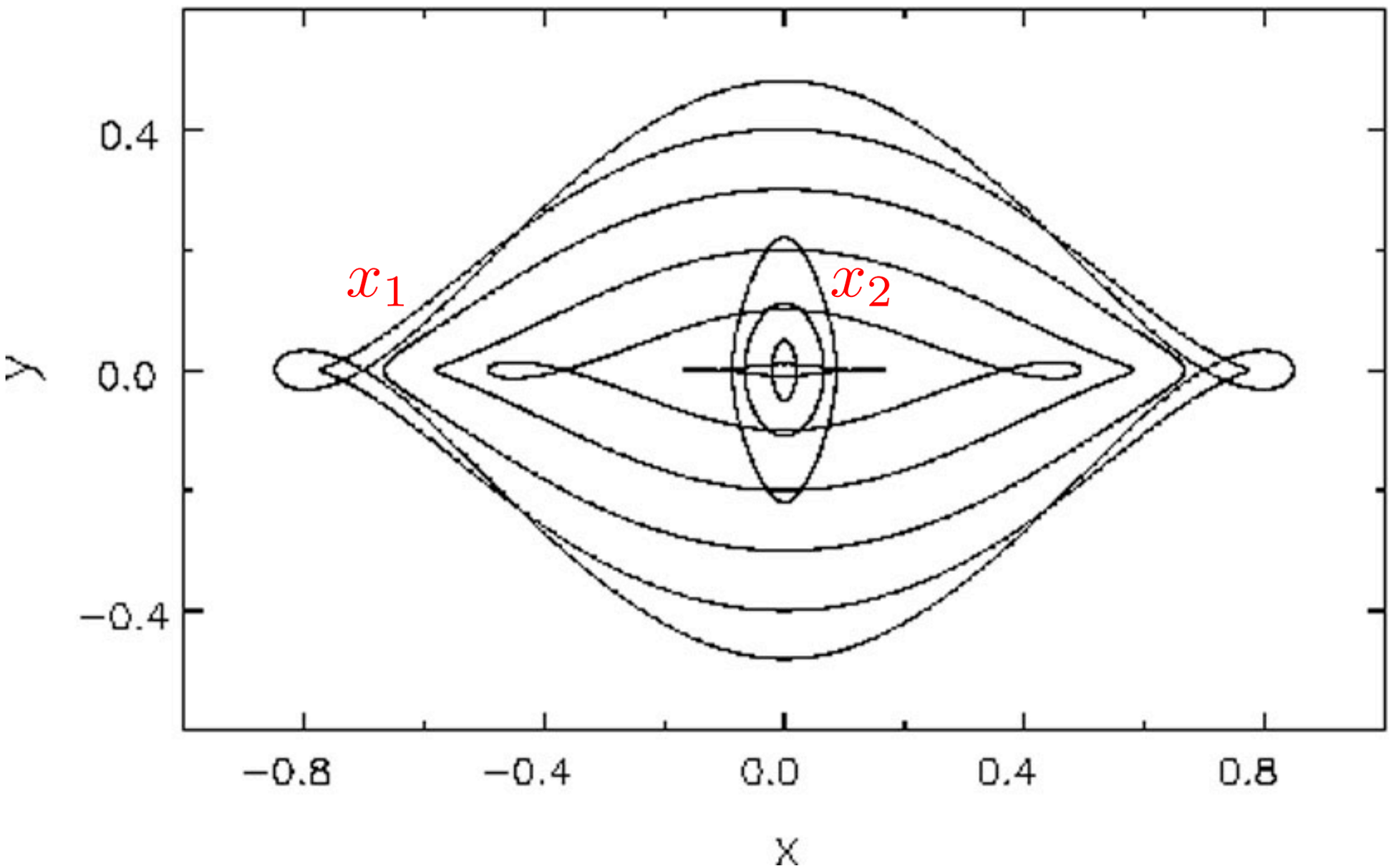

Binney et al

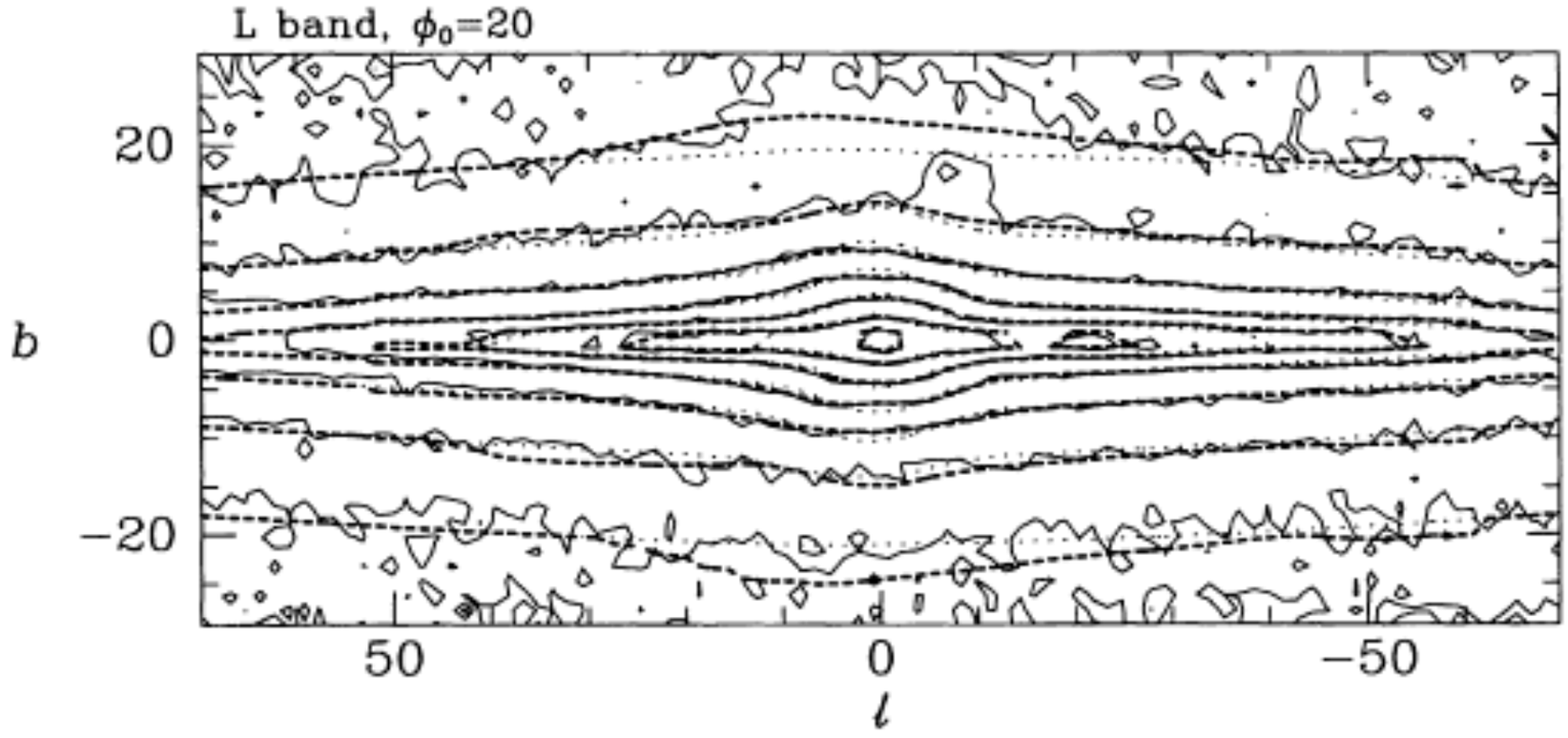

Figure 1. The fit between data (full contours) and model (thick dashed contours) that is obtained after five iterations of the Richardson–Lucy algorithm under the assumption that $\phi_0 = 20°$. The dotted contours show the initial analytic fit of equation (1). Contours are spaced by 1 mag. The Sun–centre line is assumed to lie 0.1 above the plane.

asymmetry in star counts indicates bulge is a bar

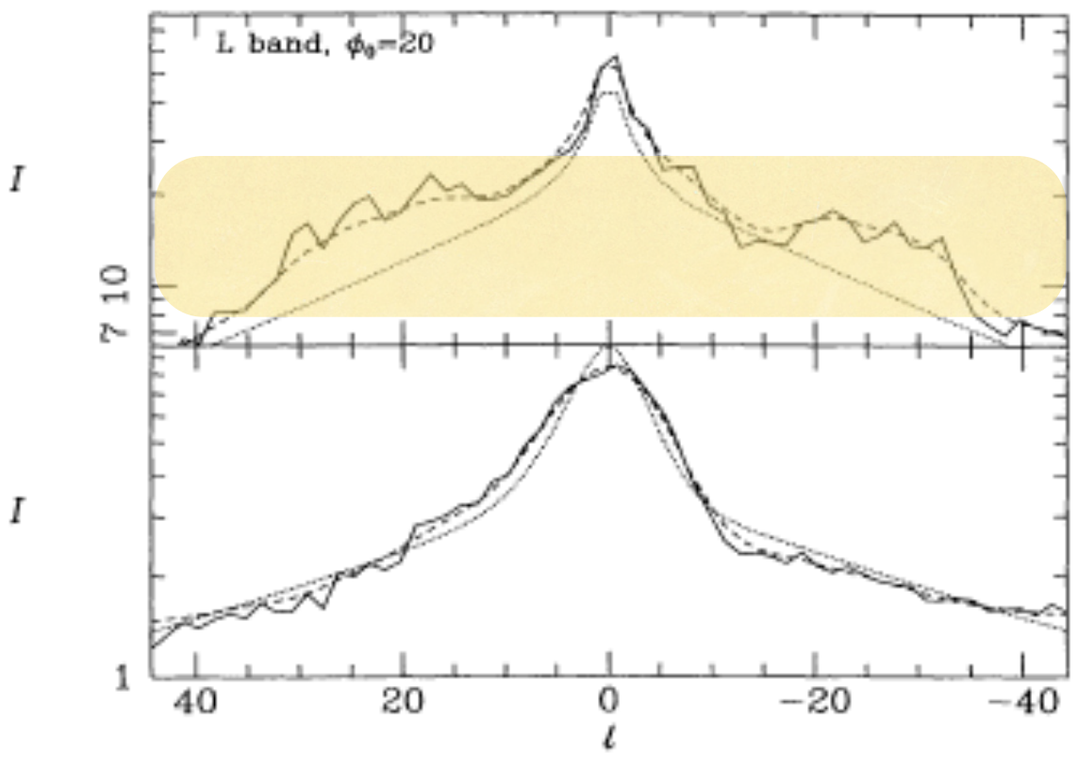

inferred by Kent et al. (1991) from Infrared Telescope data. At higher latitudes the iterations make smaller changes, but these include successfully modelling significant asymmetry in latitude at $|l| \lesssim 10°$. In fact, this figure shows that the final model fits the data nearly as well as any smooth model could, and that the remaining residuals are associated with small-scale structure which it is not appropriate to model at this stage.

The fit plotted in Figs 1 and 2 was obtained under the assumption that the Sun–centre line lies 0.1 above the assumed symmetry plane of the Galaxy. That is, the Sun has been assumed to lie 14 pc above the plane. Fig. 3 compares the residuals (model − data) that one obtains for this case with those that one obtains when the Sun is located within the plane (bottom panel) or 28 pc above the plane (top panel). Whereas in the bottom panel positive residuals tend to occur at $b > 0$, in the top panel they occur at $b < 0$. From the fact that in the middle panel positive and negative residuals show no

Gerhard (2017) arXiv:1710.01544

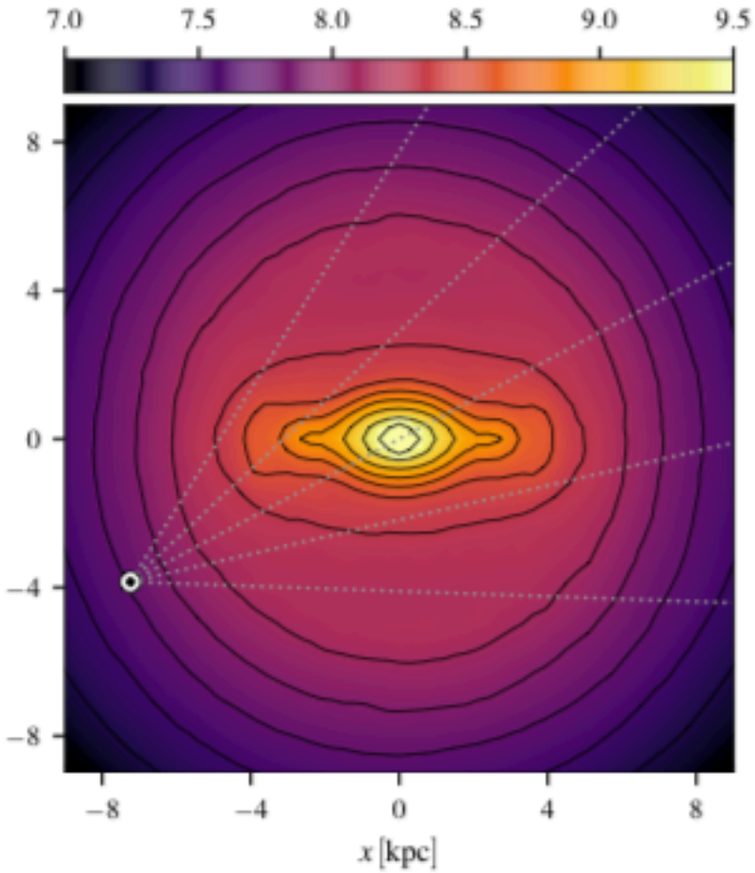

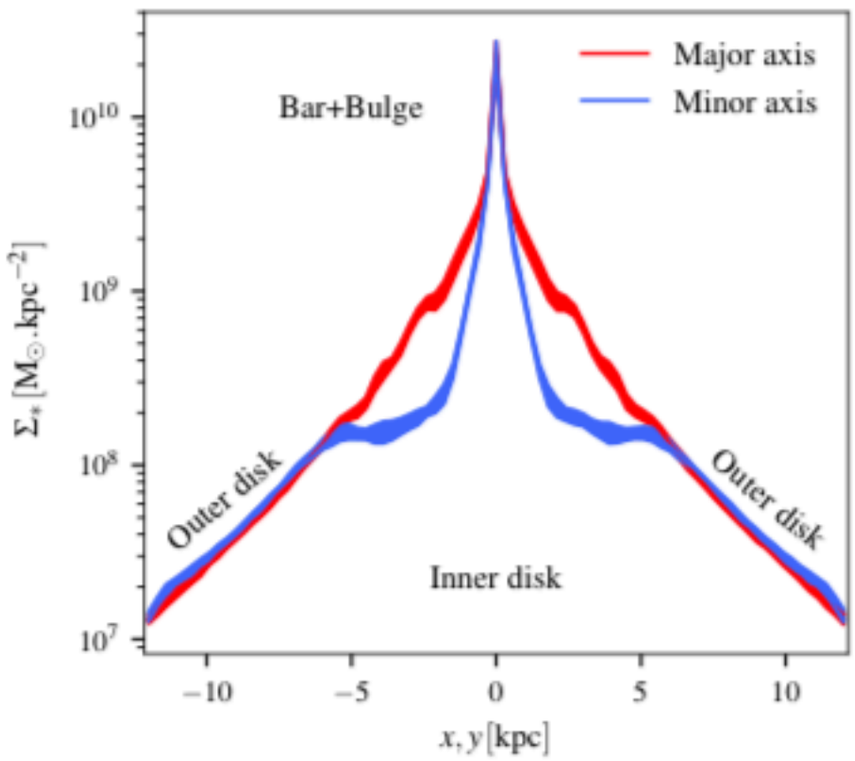

Figure 1. Face-on stellar surface density of the best Bulge and Bar model of P17a. The position of the Sun and sightlines for longitudes $l = -30°, -15°, 0, 15°, 30°$ are indicated.
Figure 2. Model surface density profiles along the major and in-plane minor axis of the Galactic Bar. Both figures adapted from Portail et al. (2017a).

Pattern speed of MW bar is estimated to be

$$\Omega_B \approx 70\ (55)\ \mathrm{km\,s^{-1}\,kpc^{-1}}$$

if corotation is at ~ 3 (4) kpc

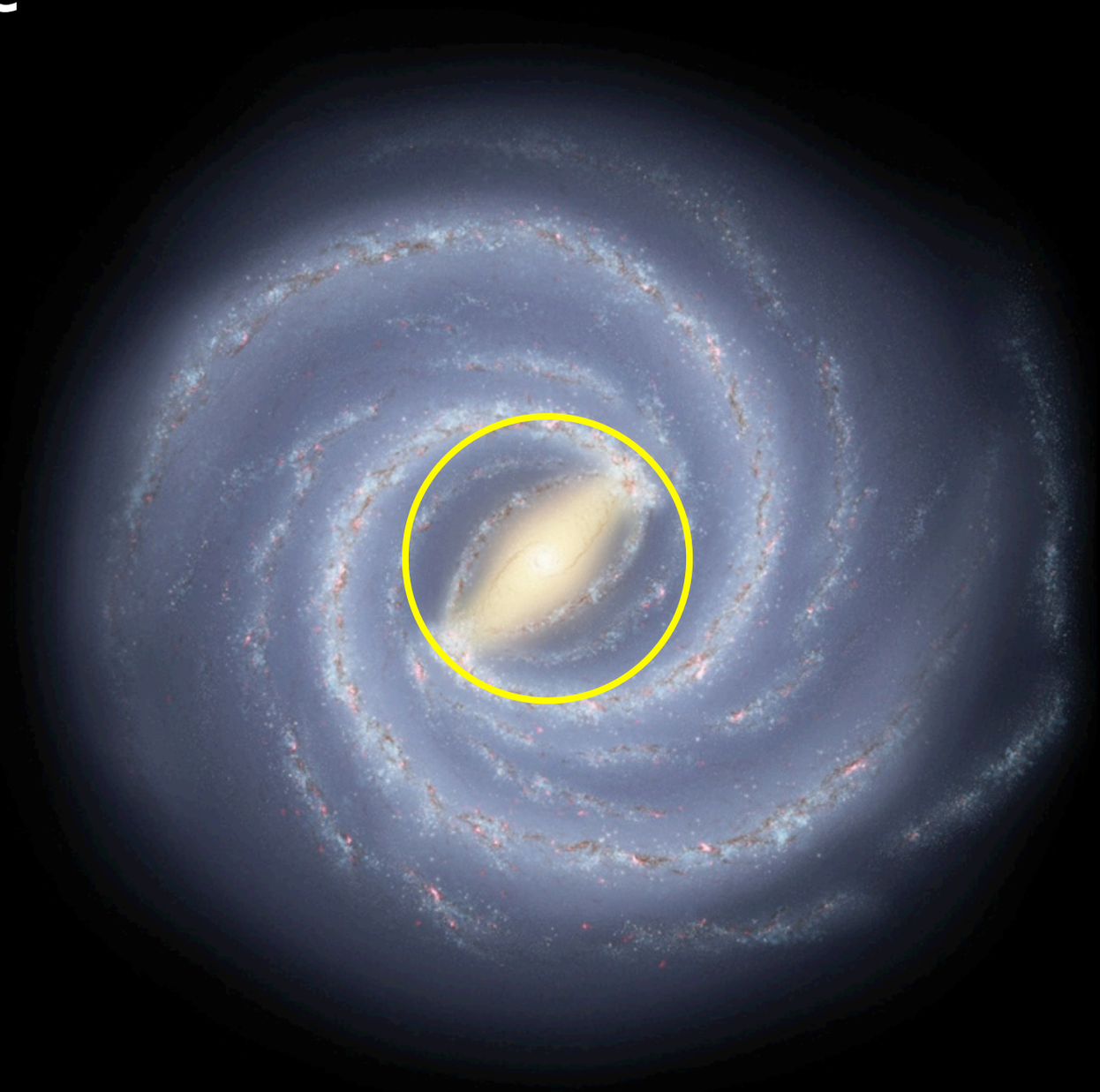

Lindblad resonances occur when

$$m(\Omega - \Omega_B) = \kappa$$

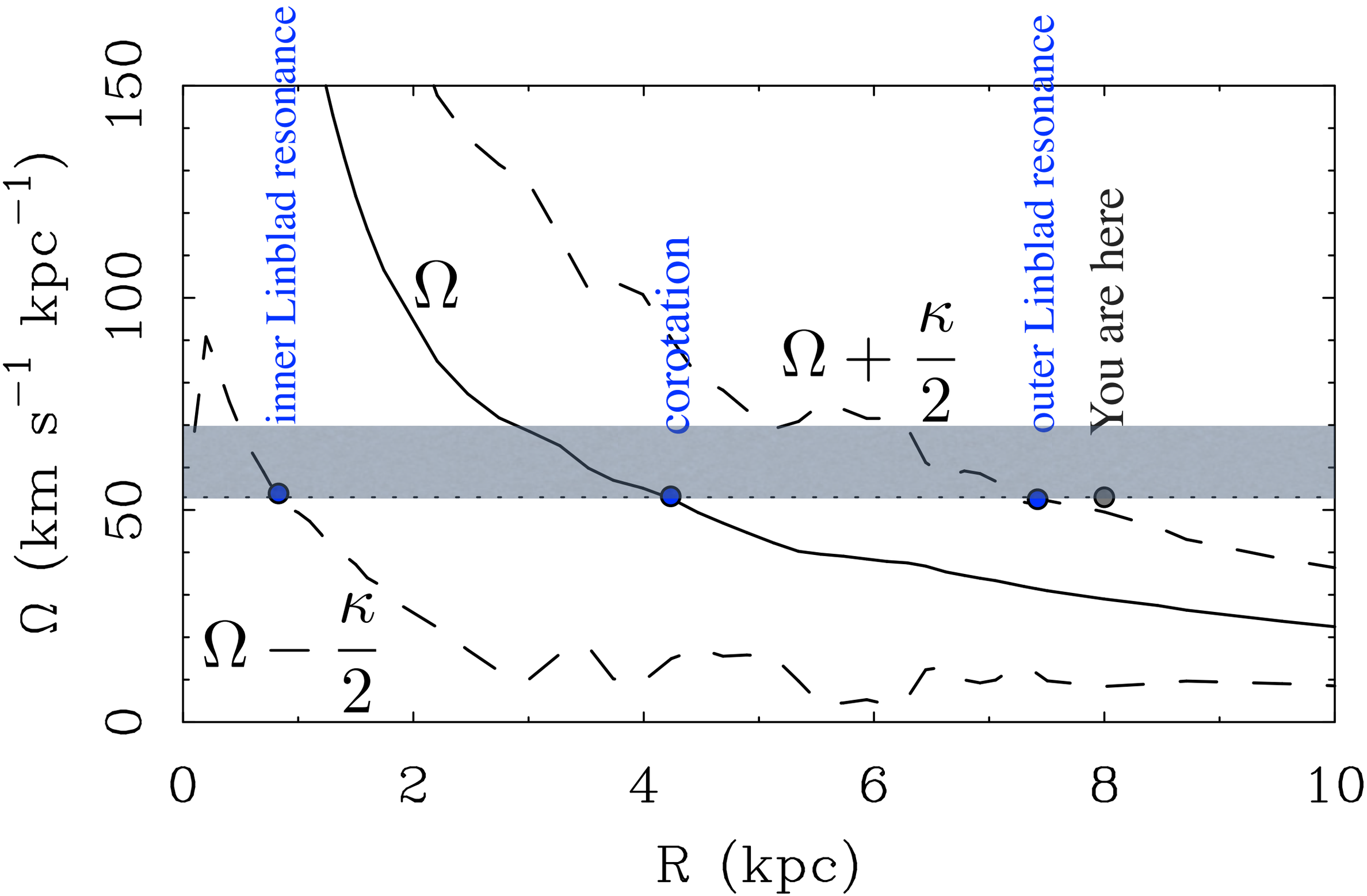

Measured bar pattern speeds

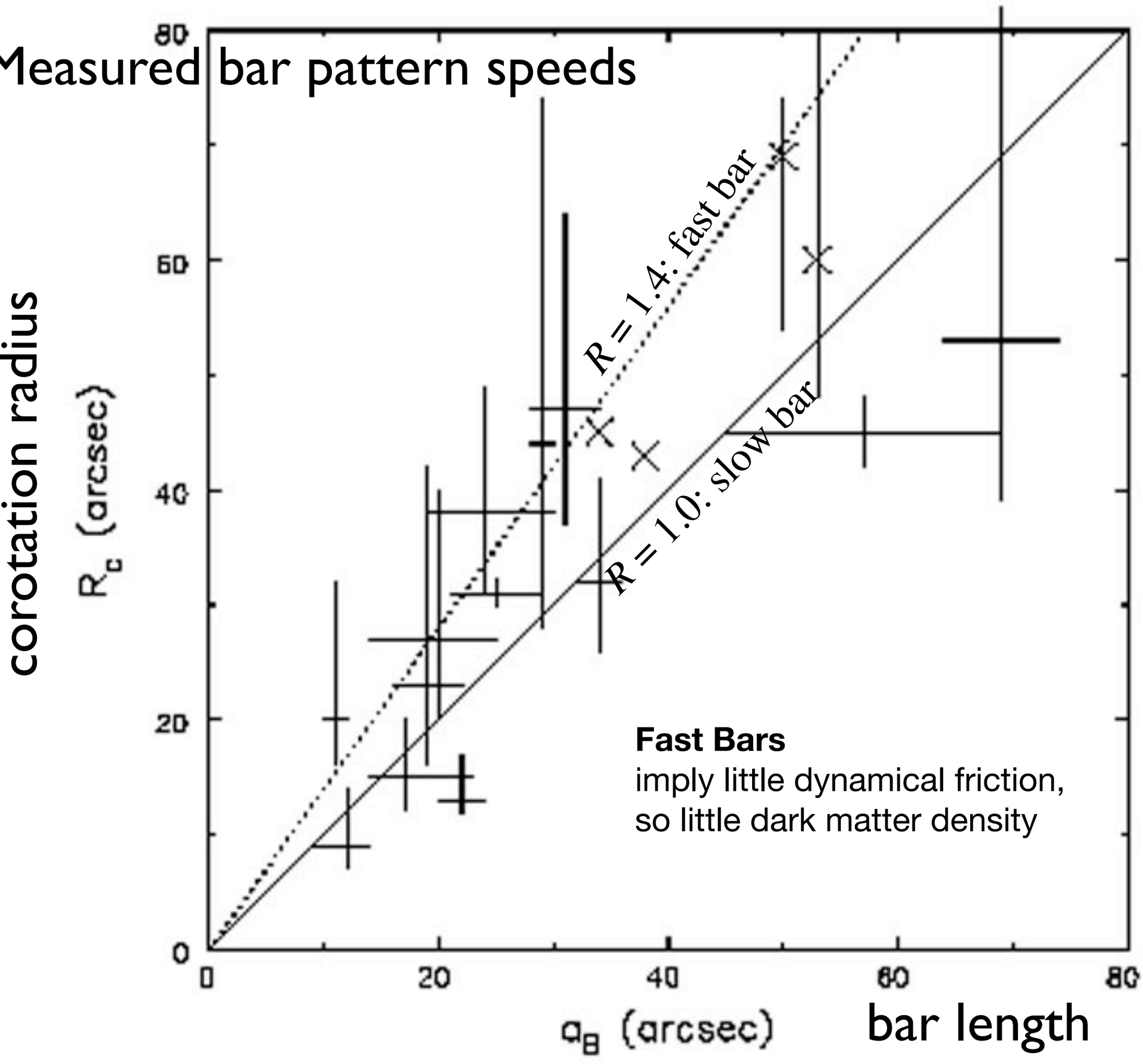

Fast Bars
imply little dynamical friction,
so little dark matter density

Disk Stability

- Dark matter halos required for stability
  - No halo: bar instability
  - Too much halo: too stable - slow bars or no bars
- Same for spiral structure
  - low modes least suppressed
  - Grand design (m=2) spiral pattern indicates substantial disk self-gravity

Spiral Structure

From swing amplification (Toomre 1981)

Growth of m=2 mode as it oscillates between the inner and outer Lindblad resonances

subject to no extra forces from an imagined halo. The fiercest of these instabilities (with pattern speed $\Omega_p = 0.4153$ and growth rate $s = 0.2178$ in obvious units) is shown developing at the usual alarming pace in Fig. 9. This mode A would be referred to as the "bar mode" by most workers — especially after its growth rate is weakened and its planform made less spiral, as in Figs. 11-12, by locking up more and more of the disk mass for the sake of argument. It is also the kind of mode which, I dare say, practically every one of us has at some time guessed to be the one most closely analogous to the principal instability of the Maclaurin spheroids.

Plausible though it seems, the Maclaurin analogy is fallacious. Erickson's mode A is in truth just the first of a long series of swing-amplified modes, each of which is indebted also to the above-mentioned return of signals via the trailing → leading density waves. One can surmise this to a fair extent already from the great family resemblance of modes A, B, C, E, F in the density plots of Fig. 10, and from the shared trends of their pattern speeds and growth rates in Fig. 11 as the "active" disk mass is progressively reduced. But the real clincher in my opinion comes in Fig. 12, which reports the modal shapes for the case where only two-thirds

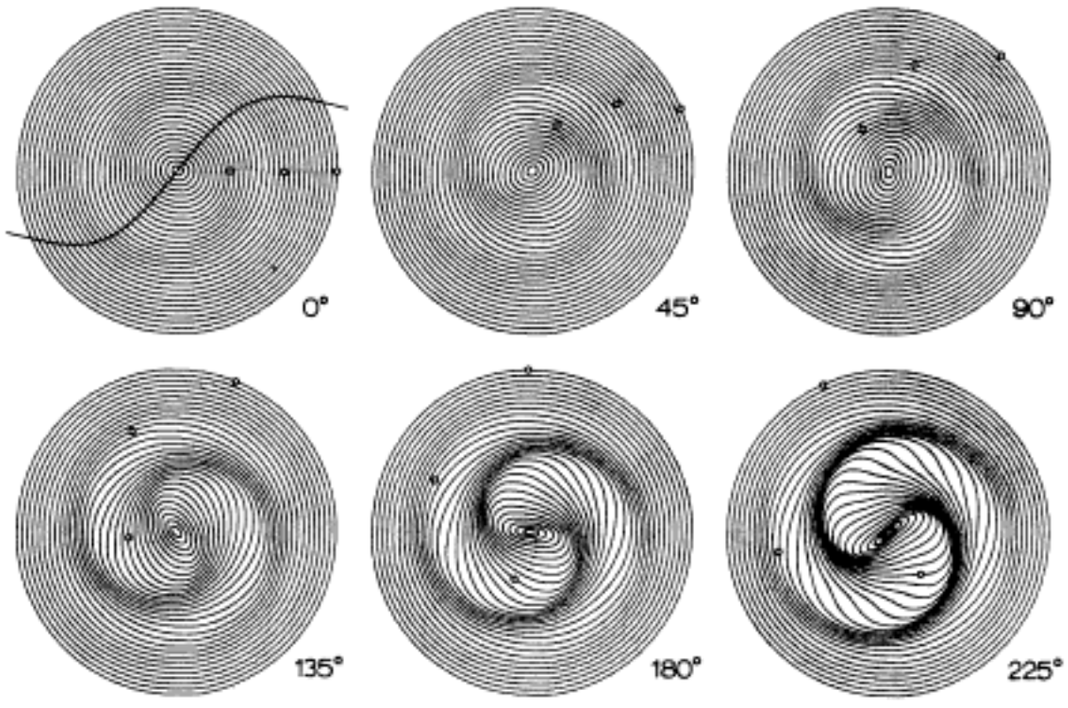

Fig. 9 Rapid growth of Erickson's (1974) dominant unstable mode A in the cold, $a = 0.25$ Gaussian disk. From frame to frame, this pattern turns exactly 45° counterclockwise, and it intensifies by a factor 1.51. Like the three marked particles from $r = 1$, 2 and 3, all constituents here orbited initially in concentric circles and shared the rotation curve superposed on the first frame.

Athanassoula et al. (1987) pointed out that a minimum amount of disk self-gravity was required to drive spiral structure, providing a lower limit on the masses of spiral disks.

$$X = \frac{r\kappa^2}{2\pi G m \mu}$$

should bracket the reality. We then obtain for each arm multiplicity an estimate of the range in radii over which amplification is permitted. The proper value of Q is not important (cf. Fig. 7 of Toomre, 1981 or Fig. 26 of Athanassoula, 1984. If the allowed $m = 1$ amplification is large we lower the $(M/L)_d$ as necessary. When a solution with no sizeable $m = 1$ is found we label it "maximum disk with $m = 1$ inhibited" or, for short, "no $m = 1$". The amplification drops sharply as the M/L is decreased (see Fig. 8 of Toomre 1981) so the range of M/L_d over which the transition from significant to no amplification occurs is relatively small. We then continue lowering the $(M/L)_d$. When we reach the point were the $m = 2$ amplification is in turn inhibited we

$MH(R_{25}/3)/MH(R_{25})$. Secondly, an isothermal sphere model is fitted to the halo velocities from which we obtain a core radius (R_c), central density (ρ_0), dispersion (σ), halo mass within R_{25} and concentration indices as above. The last fit is that of a power law to the halo density. All these quantities will be used later to parametrize the halo.

An illustration of the modelling has been reproduced in Fig. 1 for the galaxy NGC 598. Figure 1a shows the photometry data. The "maximum disk" solution is given in Fig. 1b by a solid line, together with the observed velocity data. The amplification factors for NGC 598 are plotted in Fig. 1d for both $m = 2$ and $m = 4$. For this galaxy the maximum disk solution has no $m = 1$

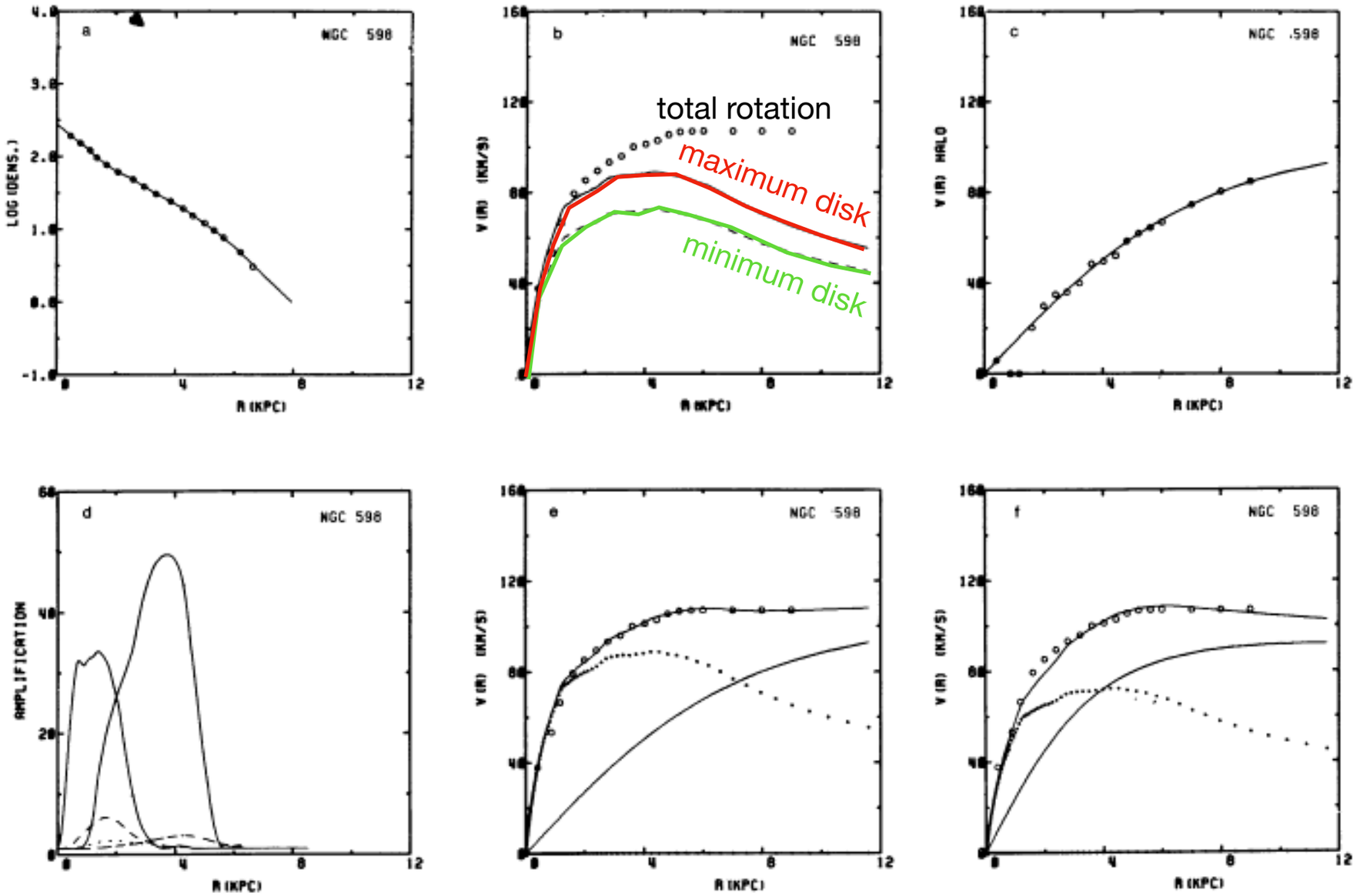

Fig. 1a–f. Mass model for M 33. **a** The radial luminosity profile taken from De Vaucouleurs (1959). **b** Rotation curves calculated for the maximum disk solution with M/L (corr) = 1.89 (solid curve), and the no $m = 2$ solution with M/L (color) = 1.24 (dashed curve). The observed rotation data (circles) have been taken from Newton (1979). **c** Isothermal sphere model fitted to the halo velocities obtained for the maximum disk solution. **d** Amplification factors as function of radius for the no $m = 1$ solution for $m = 2$ (left side) and $m = 4$ (right side). The curves are for different values of Q: 1.2 (solid lines), 1.5 (dashed lines), and 2.0 (dashed-dotted lines). **e** final composite for the no $m = 1$ solution. The disk curve, the isothermal halo fit, and the composite are shown, together with the observed data (circles). **f**, as e, but for the no $m = 2$ solution

Exponential disks in 3 dimensions

$$\rho(R, Z) = \rho_0 e^{-R/R_d} e^{-|z|/h_z}$$

R_d Radial scale length $R_d \approx 2$ to 3 kpc

h_z vertical scale height $h_z \approx 300$ pc

for external galaxies, typically $R_d/h_z \approx 6$ to 10

other models possible, e.g., $\mathrm{sech}(|z|/z_0)$

can have multiple components with different scale sizes

radial direction

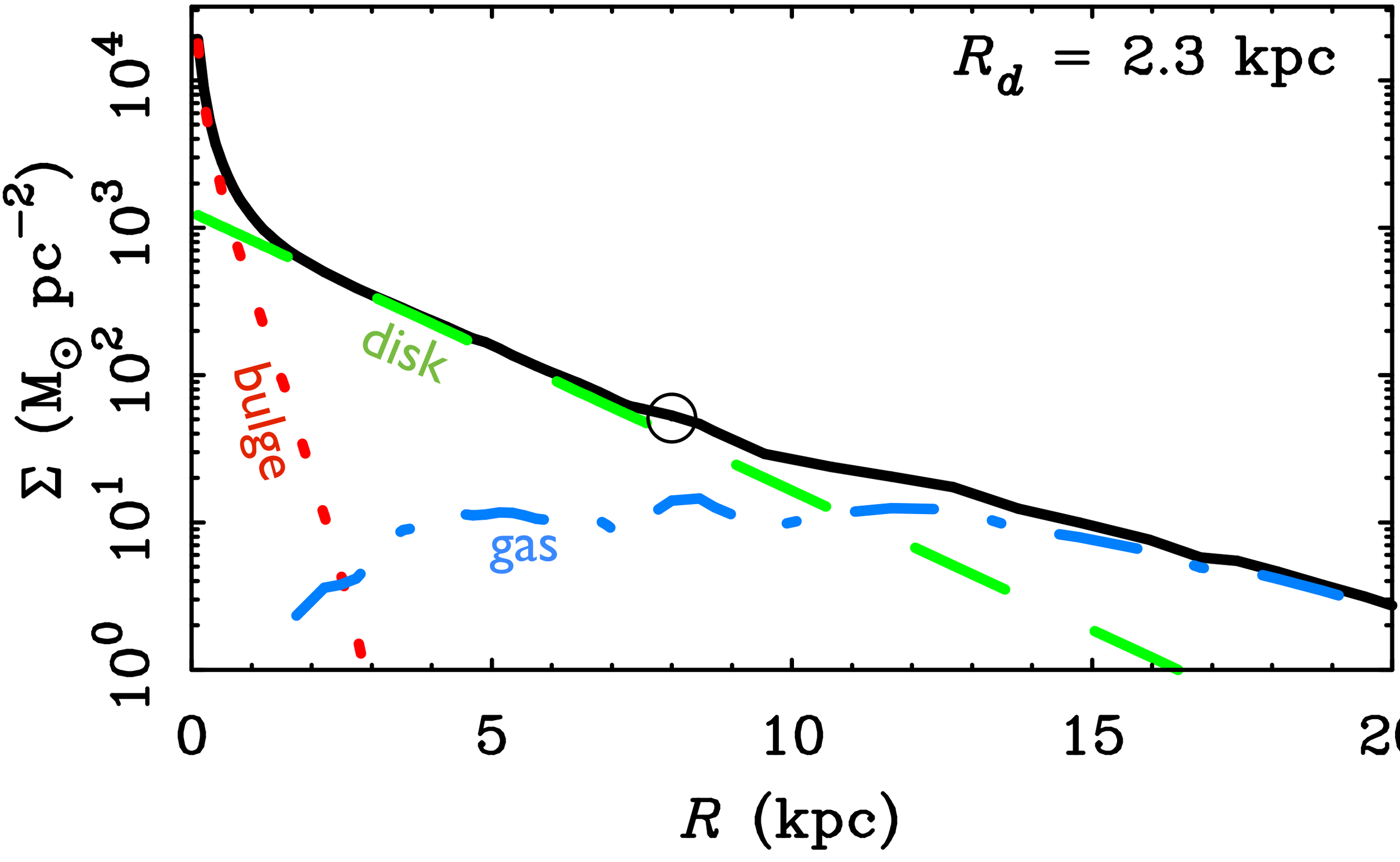

also exponential in vertical direction; scale height depends on the population

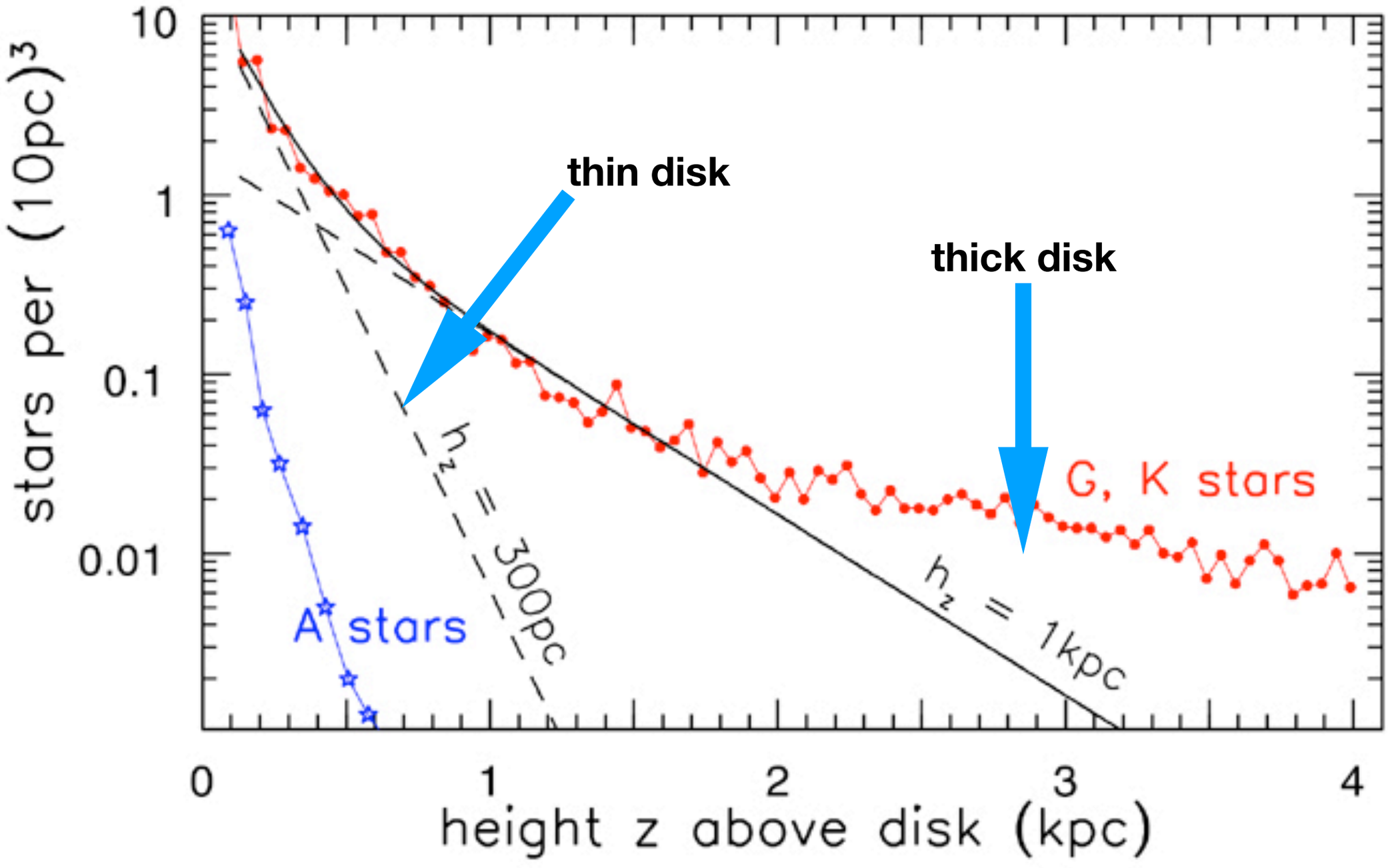

Fig 2.8 (Reid, Knude) 'Galaxies in the Universe' Sparke/Gallagher CUP 2007

<u>Thin disk</u>
Age: 8 Gyr

<u>Thick disk</u>
Age: 9.5 Gyr
mass fraction: ~20%

<u>Stellar Halo</u>
Age: 12.5 Gyr
mass fraction ~1%

Ages from oldest white dwarfs
(Mukremin et al. 2017)

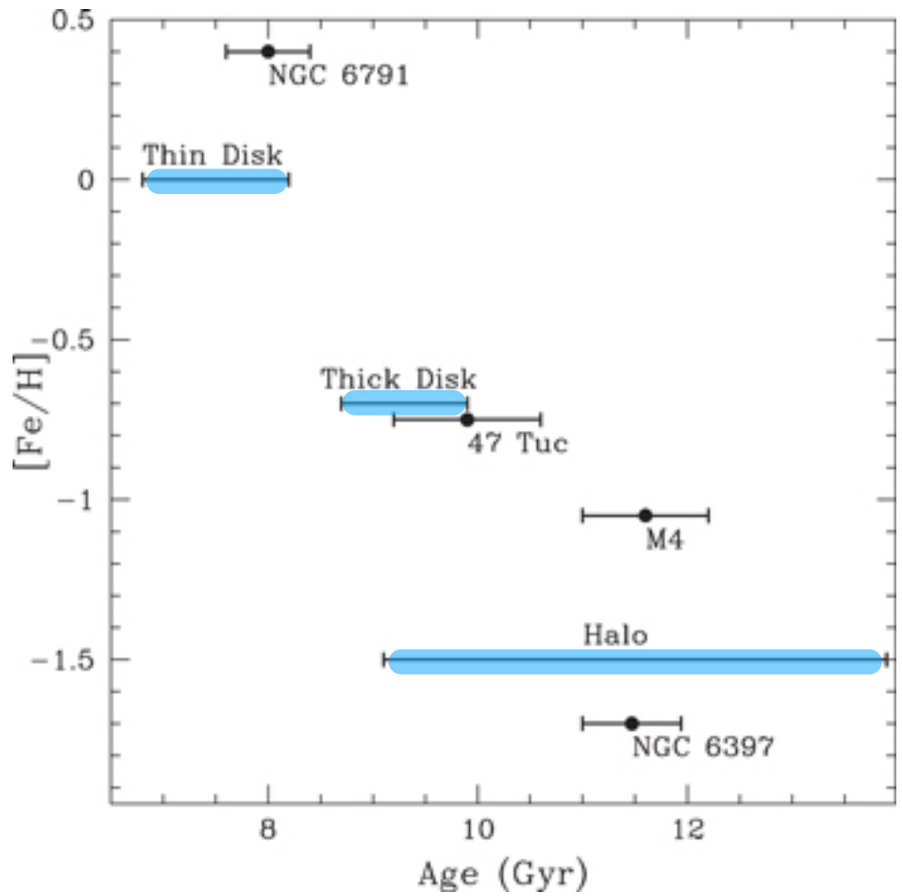

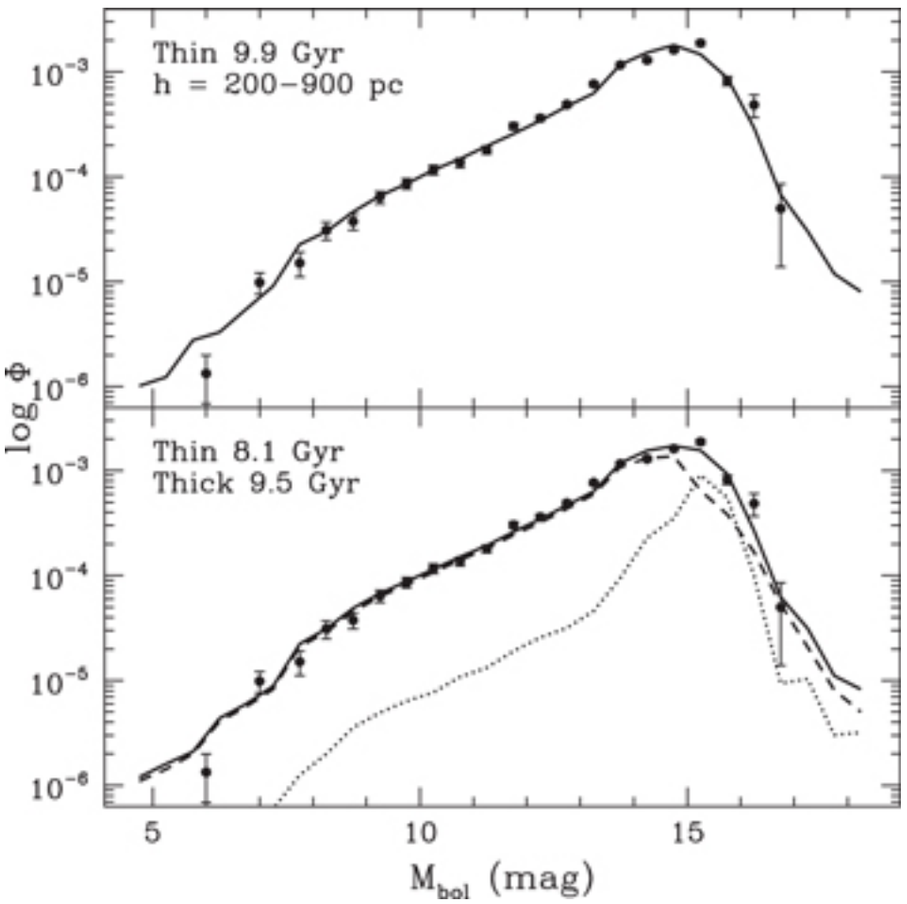

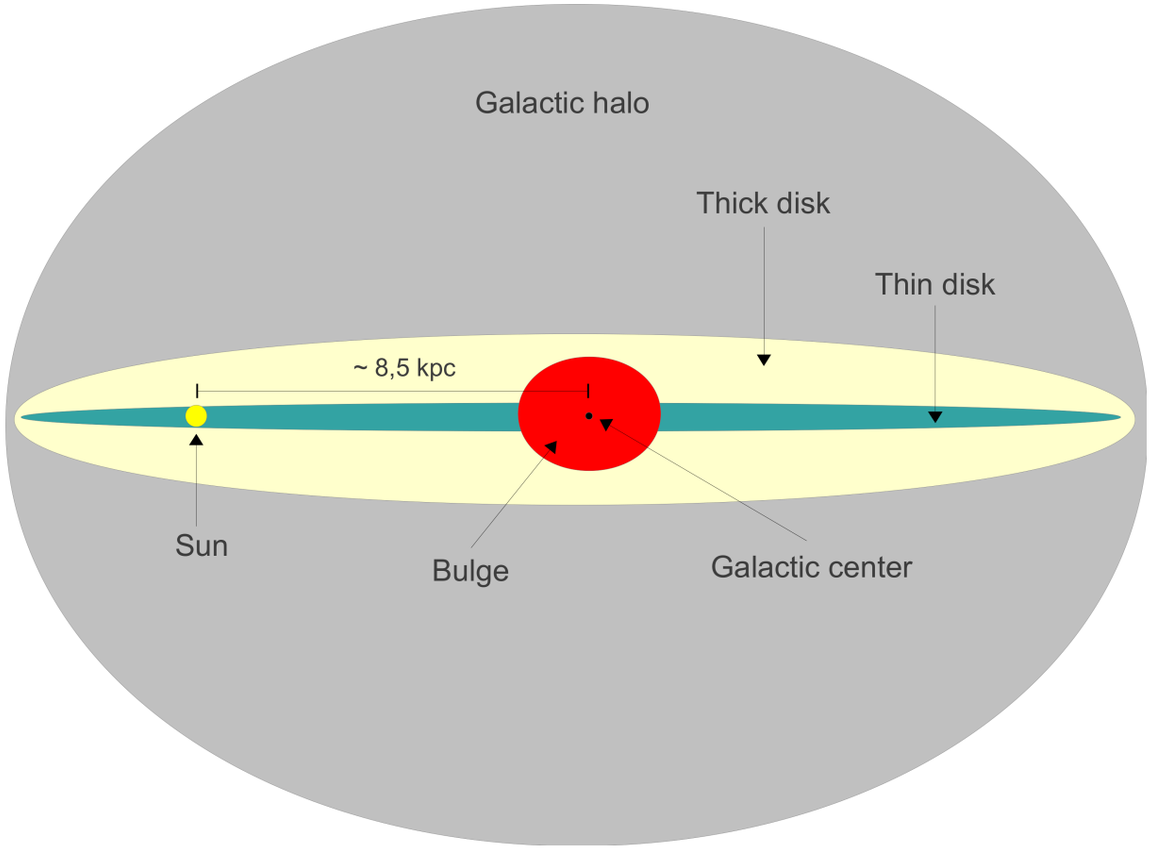

Toth & Ostriker (1992)

Mergers thicken and heat disks. The existence of cold, thin disks (spiral galaxies) limits the mass of mergers to < 1:10 (crudely speaking).

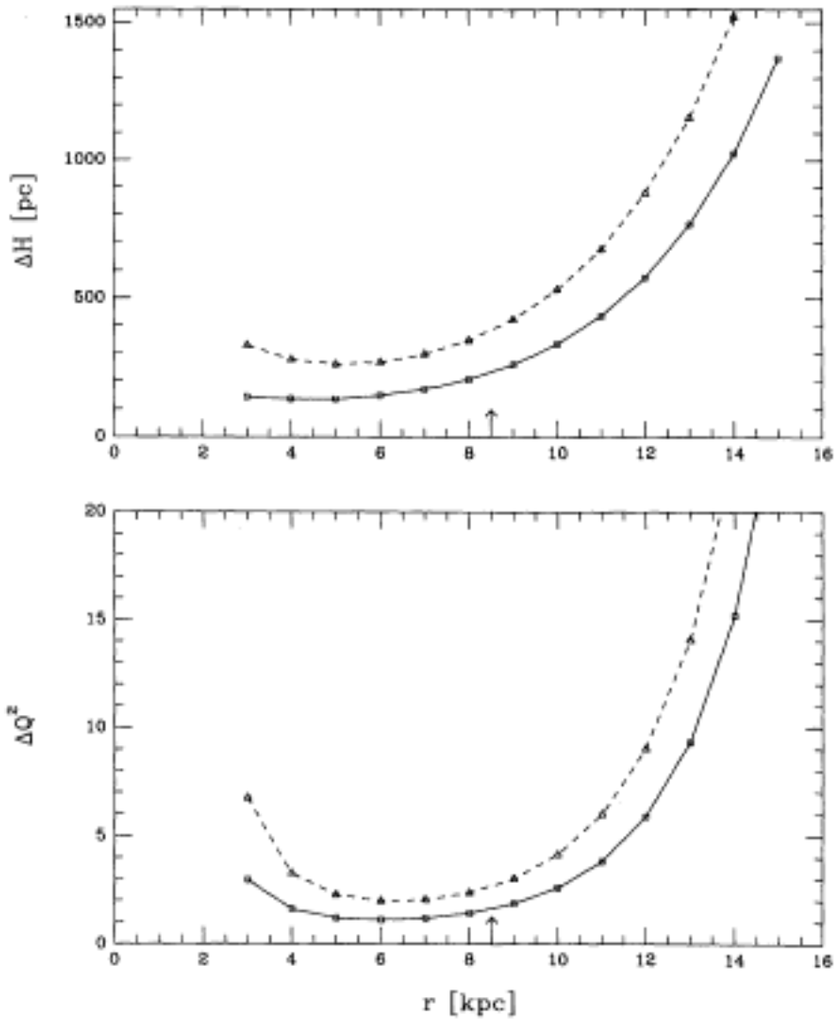

ght and Toomre's Q in the Caldwell-Ostriker galaxy model. The infalling satellites are modeled by Jaffe spheres with a total mass of the solar circle ($=4.3 \times 10^9\ M_\odot$) and scale lengths of 1 kpc (*solid lines*) or 0.1 kpc (*dashed lines*). They are assumed to spiral in along distribution of orientations. See § 4 for details. In the top panel the scale-height increase ΔH is plotted against the Galactocentric he change in Toomre's Q^2 is shown.

odds of dodging a major merger are small

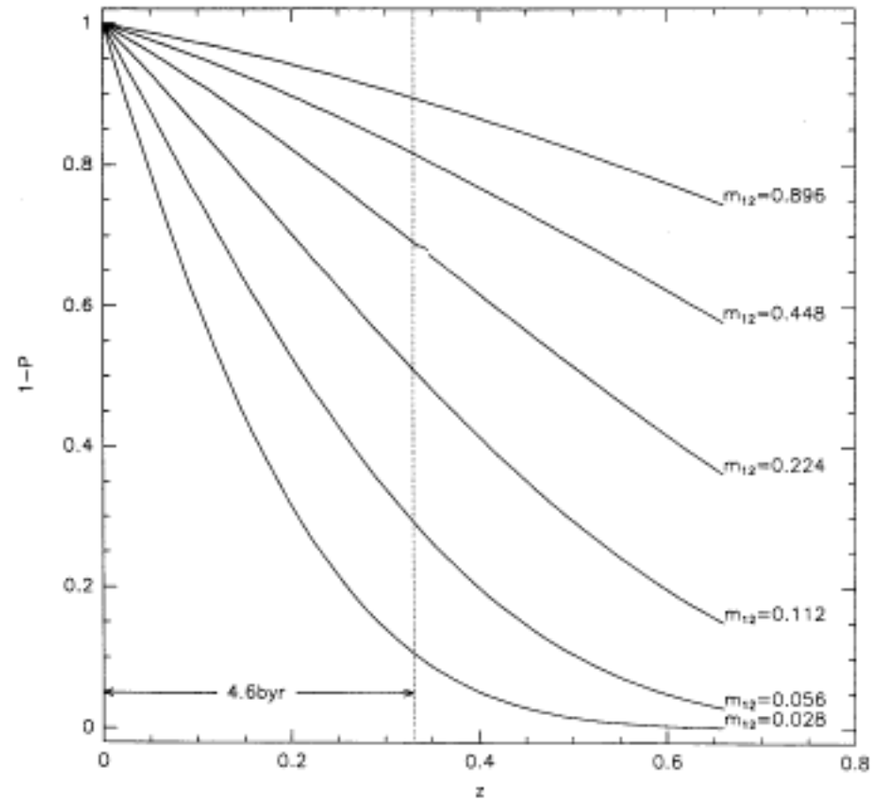

s, after Carlberg (1990b), as a function of look-back time. The typical (L_*) galaxy would have hance of a merger with one of mass $3 \times 10^{10}\ M_\odot$ within the lifetime of the Sun.

The Milky Way has an old (~9 Gyr) thick disk, that is a modest fraction of the total stellar disk mass. Perhaps a sizable merger thickened the disk long ago, but not much has happened since.

Dynamical friction acts to slow a particle of mass M and velocity v_M traversing a medium of N gravitationally attractive particles each of mass m.

consider a mass, M, moving through a uniform sea of stars. Stars in the wake are displaced inward.

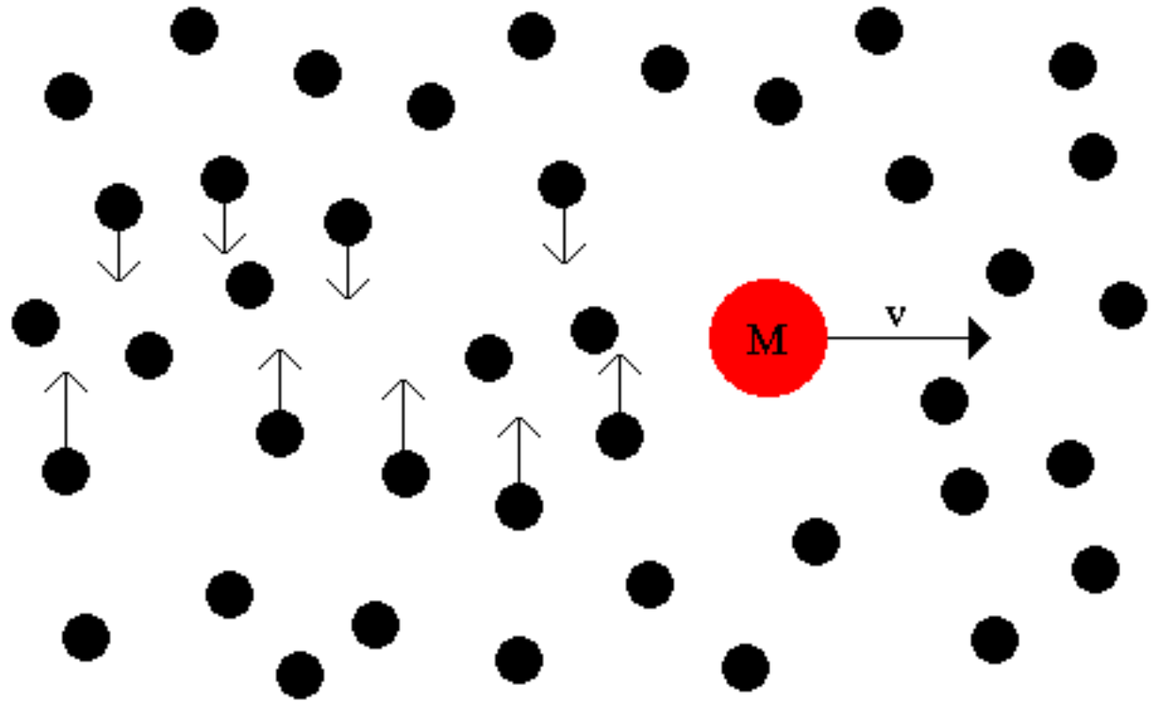

Dynamical friction arises when the passage of an object pulls particles towards it, creating a density enhancement in its wake. This density enhancement pulls back against the motion of the object.

this results in an enhanced region of density behind the mass, with a drag force, F_d known as dynamical friction

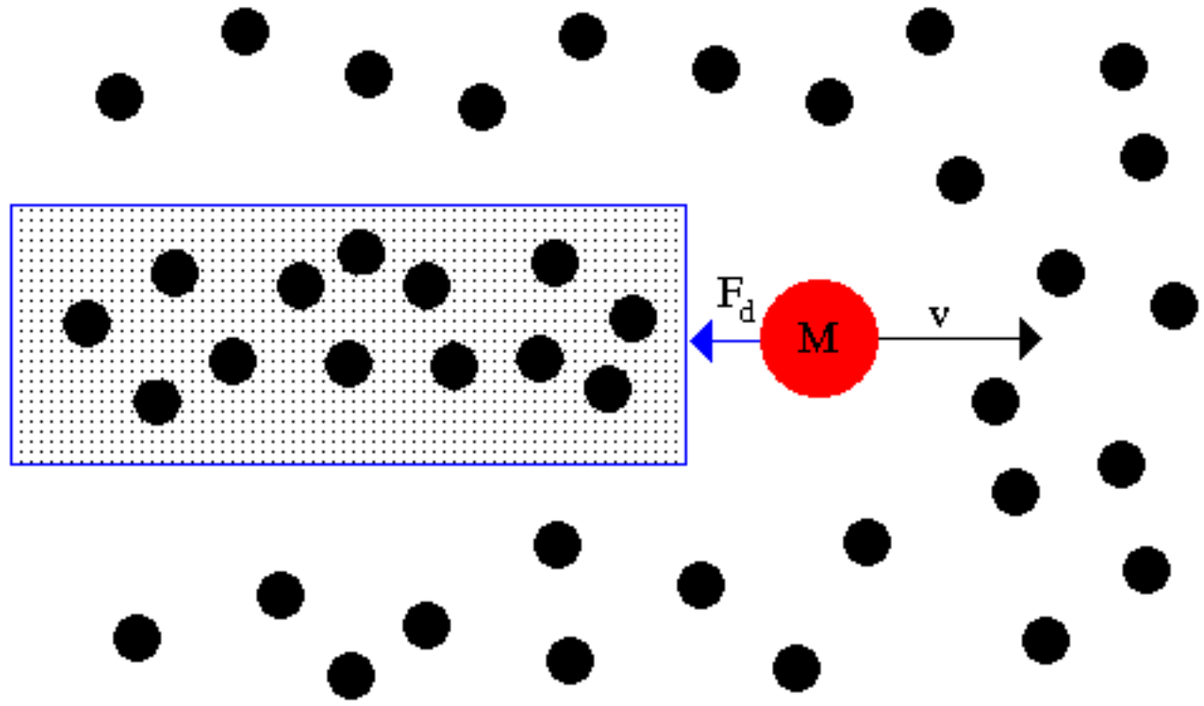

Dynamical friction acts to slow a particle of mass M and velocity v_M traversing a medium of N gravitationally attractive particles each of mass m.

Chandrasekhar formula for dynamical friction (BT eqn 8.3)

$$\frac{d\vec{v_M}}{dt} = -16\pi^2 G^2 M m \ln\Lambda \frac{\vec{v_M}}{v_M^3} \int_0^{v_M} f(v) v^2 dv$$

net frictional force

Coulomb logarithm

distribution fcn of background particles (N of mass m and velocity v)

The Coulomb logarithm measures the "extent" of the system and is a complete kludge

$$\Lambda \approx \frac{b_{max}}{b_{min}} \approx \frac{NmR}{M\mathcal{R}}$$

R ← orbital radius of mass M

$\mathcal{R}$ ← extent of N masses m
e.g., the radius of a dark matter halo

Examples where dynamical friction is important

- Dynamical friction acts to slow the pattern speed of bars embedded in dark matter halos.

Mostly. We think.

Some configurations of live halos can amplify rather than suppress bars!

- Plays a role in the orbits of satellite galaxies and their incorporation into larger dark matter halos.

- Also required for merging galaxies - orbital energy and angular momentum gets transferred to the dark matter halo, which acts like a big catchers mitt to make galaxies merge that would otherwise just fly past each other.

The Antennae [merger of NGC 4038 and NGC 4039]

Merging galaxies simulation by Prof. Mihos

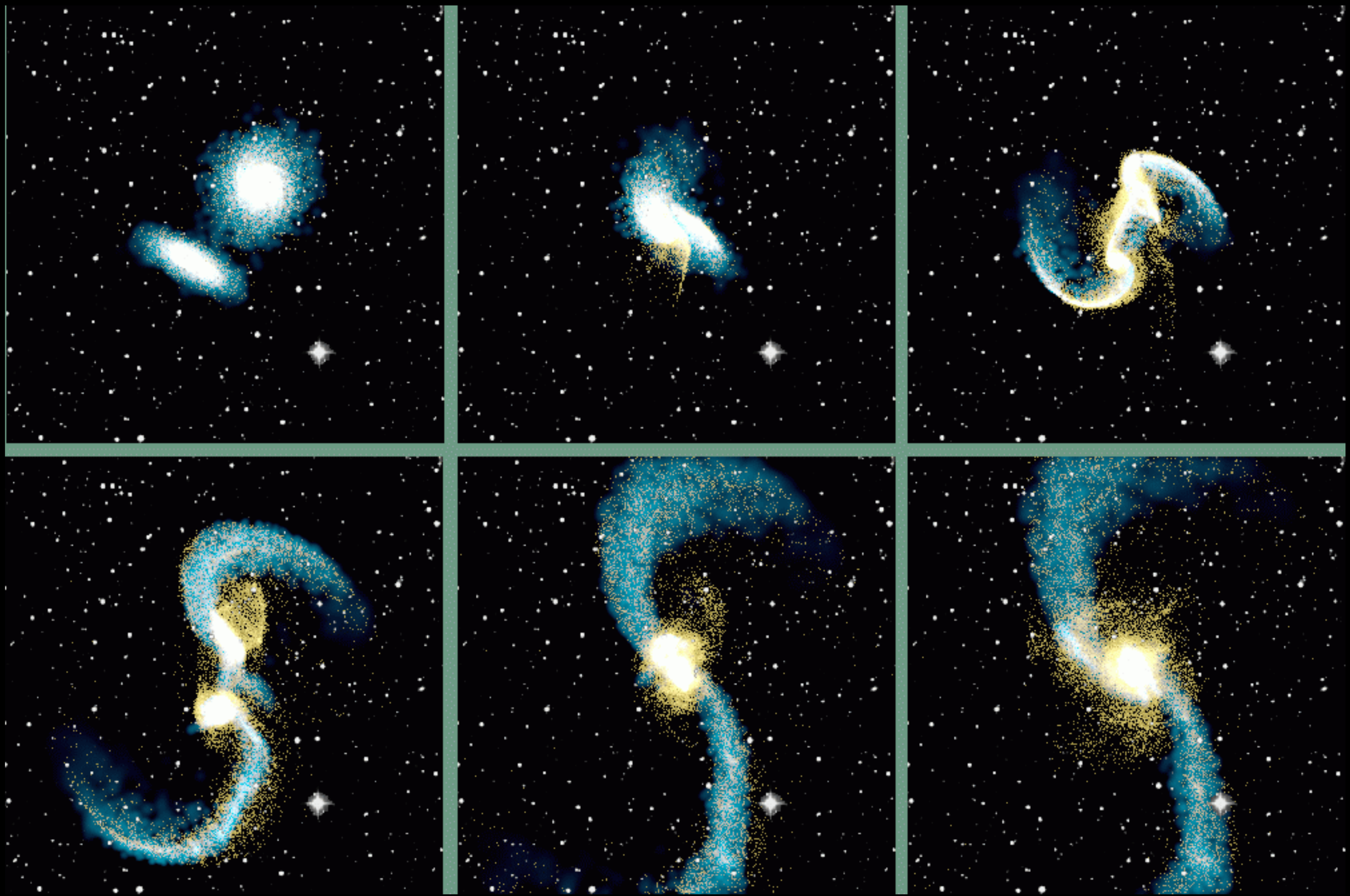

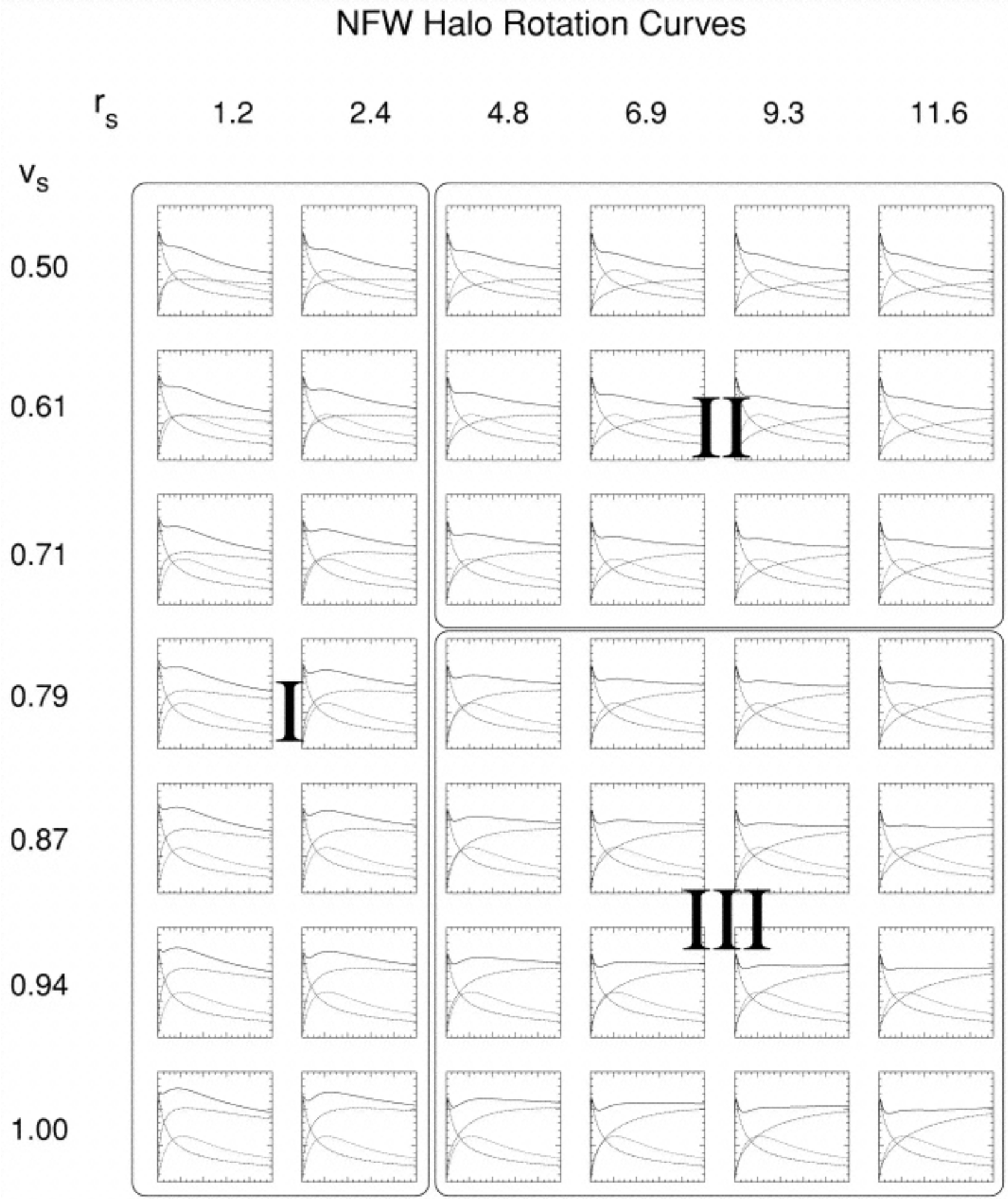

Merging galaxy models
initial rotation curves

Dubinski, Mihos & Hernquist (1999)

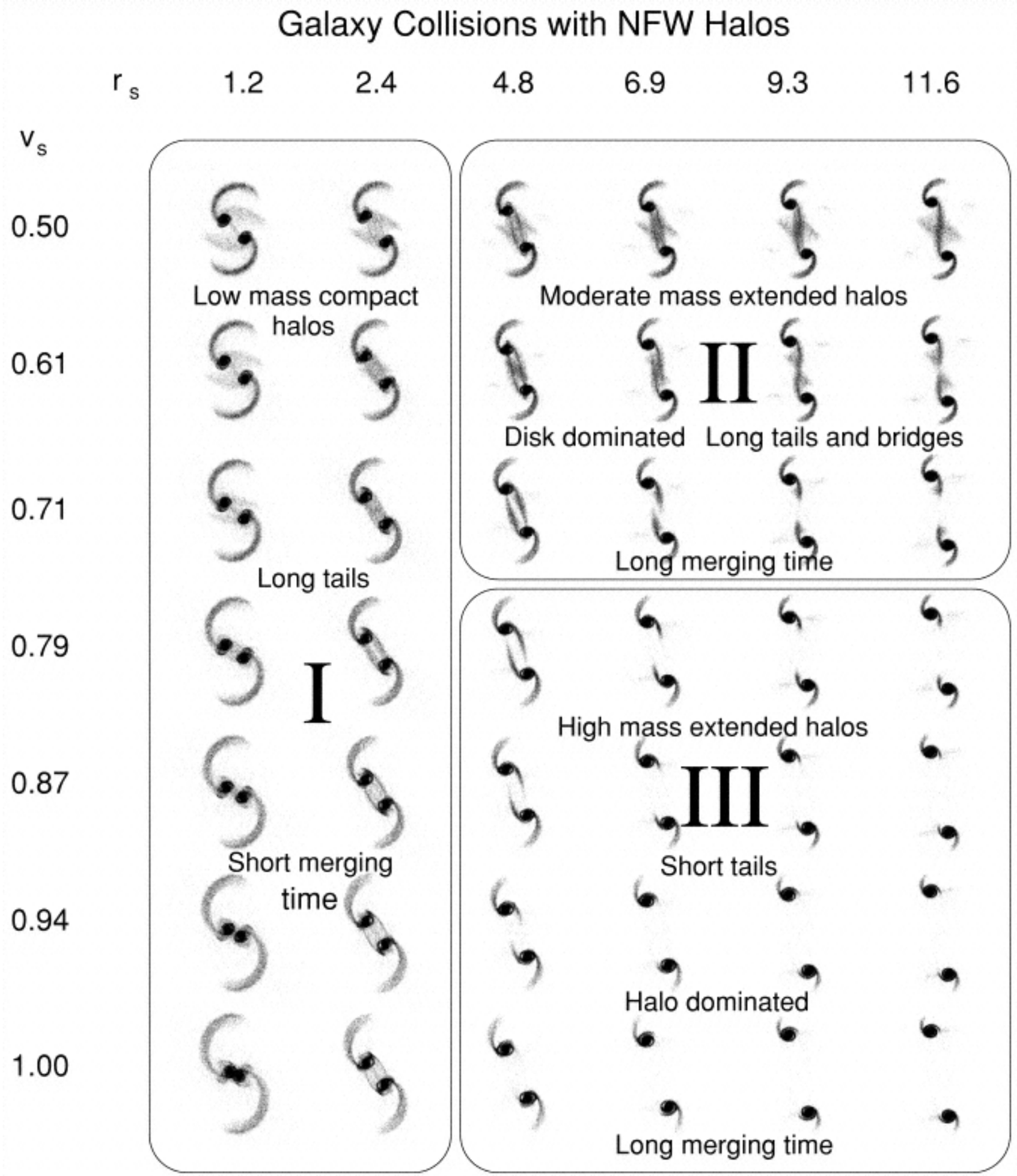

Merging galaxy models

morphology of merger models

Dubinski, Mihos & Hernquist (1999)

Zone II gives the most realistic tidal tail morphologies.

Zone III has more realistic rotation curves.

Small contradiction, that.

The potential well of the DM halo needs to be deep enough to cause a merger, but not so deep that it inhibits the formation of tidal tails.